TELKOMNIKA Telecommunication, Computing, Electronics and Control
Vol. 19, No. 1, February 2021, pp. 277~284
ISSN: 1693-6930, accredited First Grade by Kemenristekdikti, Decree No: 21/E/KPT/2018
DOI: 10.12928/TELKOMNIKA.v19i1.16247

Pulse-width modulation direct torque control induction motor drive with Kalman filter

Hau Huu Vo[1], Dung Quang Nguyen[2], Quang Thanh Nguyen[3], Chau Si Thien Dong[4], Thinh Cong Tran[5], Pavel Brandstetter[6]
[1,4]Modeling Evolutionary Algorithms Simulation and Artificial Intelligence, Faculty of Electrical and Electronics Engineering, Ton Duc Thang University, Ho Chi Minh City, Vietnam
[2,3,5]Faculty of Electrical and Electronics Engineering, Ton Duc Thang University, Vietnam
[6]Faculty of Electrical Engineering and Computer Science, VSB–Technical University of Ostrava, Czech Republic

Article Info

Article history:

Received Apr 4, 2020
Revised May 19, 2020
Accepted Sep 30, 2020

Keywords:

Direct torque control
Induction motor drive
ITAE performance index
Kalman filter
Pulse-width modulation

ABSTRACT

The paper deals with application of Kalman filter in induction motor drive using pulse-width modulation direct torque control (PWM-DTC). In the first part, the conventional PWM-DTC drive is described and Kalman filter is utilized to filter components of stator current vector those are assumed to be disturbed by white noise. The second part contains simulation results that are obtained in different cases of load torque, process and measurement noise covariances. The integral time absolute error (ITAE) performance index, undershoot, ripple of important quantities are used to compare the conventional drive structure and proposed drive structure with Kalman filter. The simulation results confirm the expected dynamic response of the proposed structure.

Corresponding Author:

Hau Huu Vo
Modeling Evolutionary Algorithms Simulation and Artificial Intelligence
Faculty of Electrical and Electronics Engineering
Ton Duc Thang University
19 Nguyen Huu Tho Street, Tan Phong Ward, District 7, Ho Chi Minh City, Vietnam
Email: vohuuhau@tdtu.edu.vn

1. INTRODUCTION

Induction motors (IMs) are used in many industrial applications with wide power range from several hundreds to multi-megawatts drives because they are robust and own low cost/power and high power/weight ratios [1]. Two strategies of electromagnetic torque control: vector control (VC) and direct torque control (DTC) can be used in high precision adjustable-speed IM drives. These strategies give comparable properties. Direct torque-controlled drives were introduced more than 10 years later than vector-controlled drives [2]. The advantage of the DTC methods is their simple control structures that directly control the torque without many frame transformations [3], and therefore, they are simple to simulate on computers and easy to implement on practical control systems. DTC strategy brings desired electromagnetic torque control and robustness for controlled systems [2]. There are many versions of DTC such as Takahashi's DTC method (T-DTC) [4-6], method with dividing locus of stator flux phasor into twelve sectors (TS-DTC) [7], method that voltage vector components are proportional to deviations of flux and torque (DVC-DTC) [8], pulse-width modulation direct torque control (PWM-DTC) [2].

The switching frequency is always constant with PWM-DTC. Besides that, the PWM technique also ensures the reliable IM excitation and limitation of the stator current vector, reduces switching losses, ripple of flux and torque [9]. Current sensors are important parts of DTC drive structures, and processed by suitable algorithms. In the paper, components of stator current vector are assumed to be distorded by white noises, and in such cases, Kalman filters seem to be the most effective tools.

Kalman filter (KF) which was invented 60 years ago [10, 11], was applied to smooth noised quantities in various fields [12] for example charging state estimation of large-scale battery energy storage systems [13], mobile robot navigation [14], impedance parameters estimation for medium transmission line [15], estimation of the angle between receiver orientation and receiver-transmitter line in LED communication system [16], wildfire progress estimation [17], dimension reduction in X-ray reconstructions of undersampled dynamic X-ray tomography system [18]. The Kalman filter brings the optimal estimators for linear systems with additive independent Gaussian process and measurement noises. In practice, most control systems are nonlinear, extended Kalman filter (EKF) which utilizes Taylor series expansions to linearize a nonlinear dynamical model about a working point was made [19]. For highly nonlinear systems, unscented Kalman filter (UKF) uses the principle that a set of discretely sampled points can be utilized to parameterize mean and covariance without linearization steps [20]. In case of unknown or highly non-Gaussian inputs for linear systems, Kitanidis Kalman filter (KKF) was developed [21]. Extended version of Kitanidis Kalman filter (EKKF) for nonlinear systems has been also used for state and parameter estimation [22]. State and noise covariance matrices in EKF were selected by differential evolution algorithms [23]. In design of stator current Kalman filters, discrete-time models of induction generator were obtained by utilizing Euler difference method [24, 25]. Flux and speed are estimated using flux models-based EKF [26]. Faults detection are implemented by an IM model-based EKF [27]. Genetic algorithm is combined with an IM model-based EKF to tune noise matrices [28]. Cubature Kalman Filter estimates load torque using IM state space model [29]. An IM model-based adaptive algorithm is added to update system noise covariance matrix in EKF [30]. Speed, load torque, and efficiency are estimated by an IM model-based EKF [31]. Stator currents, rotor fluxes, load including viscous friction are estimated using EKF and UKF algorithms [32]. In the paper, primitive KF is utilized for the filtration of stator current vector components in case of unknown IM model. The paper is organized in the section structure: introduction-control structure of induction motor drive using Kalman filter-simulation results-conclusions.

2. CONTROL STRUCTURE OF INDUCTION MOTOR DRIVE USING KALMAN FILTER

Figure 1 shows the proposed IM drive structure using Kalman Filter. This structure is modified from one in [2]: with insertion of KF block between T3/2 block and signal calculation block. The block computes orienting angle γ, magnitude of stator flux vector ψ_s, and electromagnetic torque T_e according to (1-5):

$$\psi_{s\alpha} = \int \left(u_{s\alpha} - R_s i_{s\alpha\_F}\right) dt \tag{1}$$

$$\psi_{s\beta} = \int \left(u_{s\beta} - R_s i_{s\beta\_F}\right) dt \tag{2}$$

$$\gamma = tan^{-1}\left(\psi_{s\alpha}/\psi_{s\beta}\right) \tag{3}$$

$$\psi_s = \sqrt{\psi_{s\alpha}^2 + \psi_{s\beta}^2} \tag{4}$$

$$T_e = 1.5p\left(\psi_{s\alpha} i_{s\beta\_F} - \psi_{s\beta} i_{s\alpha\_F}\right) \tag{5}$$

In Figure 1, Kalman filter is used to estimate stator current vector components, and other blocks were described in [2]. Because of unknown IM mathematical model, the evolution of these components from time $k-1$ to time k is simplified according to (6):

$$x_k = F x_{k-1} + w_{k-1} \tag{6}$$

where $x = [i_{s\alpha} \quad i_{s\beta}]^T$: state vector, F is the state transition matrix applied to the previous state vector x_{k-1}, w_{k-1} is the noise vector that is assumed to be zero-mean Gaussian with the covariance $Q = \sigma_P^2 I$. The relationship between the state vector and its measurement y at the current time step k is expressed by:

$$y_k = H x_k + v_k \tag{7}$$

where H is the measurement matrix, v_k is the measurement noise vector that is assumed to be zero-mean Gaussian with the covariance $R = \sigma_M^2 I$. Prediction and update stages of Kalman filter algorithm are computed according to (8), (9) and (10-13) respectively:

$$\tilde{x}_k = F\hat{x}_{k-1} \quad (8)$$

$$\tilde{P}_k = F\hat{P}_{k-1}F^T + Q \quad (9)$$

$$\tilde{z}_k = y_k - H\tilde{x}_k \quad (10)$$

$$K_k = \tilde{P}_k H^T \left(H\tilde{P}_k H^T + R\right)^{-1} \quad (11)$$

$$\hat{x}_k = \tilde{x}_k + K_k\tilde{z}_k \quad (12)$$

$$\hat{P}_k = (I - K_k H)\tilde{P}_k \quad (13)$$

where $\hat{x}$: estimated state vector; and $\tilde{x}$: predicted state vector.

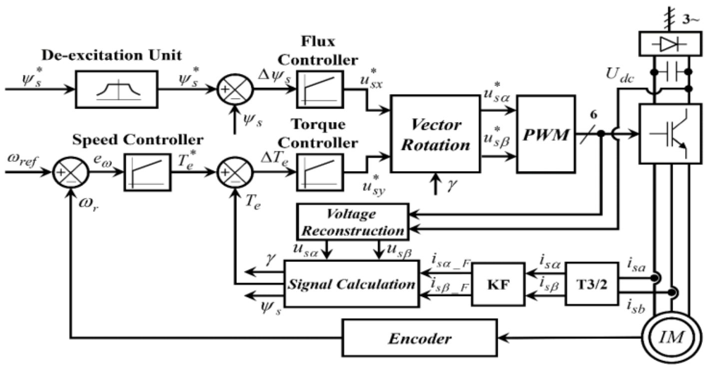

Figure 1. Control structure of PWM-DTC IM drive with Kalman filter

3. SIMULATION RESULTS

Two drive structures without and with Kalman filtering were simulated using Matlab-Simulink. Table 1 lists parameters of simulated induction motor. In order to obtain rated voltage, DC link is chosen with voltage Vdc = 540 V. Speed controller has proportional gain K_P = 1.5, integral time constant T_I = 0.05 s, limits of output ±10 Nm. The controller is tuned by finding critical value of the proportional component [33], and the integral component of the speed controller is set to zero whenever one of two limits of reference torque is reached. The switching frequency of space vector PWM is 20 kHz. Time graphs of physical quantities were archieved from the simulated structures at the jump of load torque J_{TL} (see Figure 2) in case of different values of σ_P^2 and σ_M^2.

Table 1. Parameters of simulated induction motor

Parameter	Value
Rated power	2.2 kW
Rated speed	1420 rpm
Rated voltage	230 V/400 V
Rated torque	14.8 Nm
Number of pole pairs	2
Moment of inertia	0.0047 kg m^2
Stator resistance	3.179
Stator inductance	0.209 H
Magnetizing inductance	0.192 H
Rotor resistance	2.118
Rotor time constant	0.0987s

The integral time absolute error (ITAE) for two IM drive structures are listed in Tables 2-8. For simplicity, abbreviations KF, NF respectively denote drive structures with Kalman filtering and without Kalman filtering. In most cases, ITAE for KF is smaller than that for NF. There are 14 cases that ITAE for KF is larger than 75% of that for NF, they all are with small values of σ_P^2 and σ_M^2. There are 120 cases that ITAE for KF is smaller than a half of that for NF, especially in Table 8, ITAE for KF is only 5.3% of that for NF in case of $\sigma_P^2 = \sigma_M^2 = 2$. Courses of speed and torque, stator current, and stator flux in the case are shown in Figures 3-5.

Table 2. ITAE in case of J_{TL} = 0 Nm

	$\sigma_P^2=0$, NF	$\sigma_P^2=0$, KF	$\sigma_P^2=0.25$, NF	$\sigma_P^2=0.25$, KF	$\sigma_P^2=0.5$, NF	$\sigma_P^2=0.5$, KF	$\sigma_P^2=1.0$, NF	$\sigma_P^2=1.0$, KF	$\sigma_P^2=2.0$, NF	$\sigma_P^2=2.0$, KF
$\sigma_M^2=0$	0.0349	0.0346	0.0725	0.0377	0.1239	0.0455	0.2322	0.0636	0.4565	0.1069
$\sigma_M^2=0.25$	0.0741	0.0436	0.1253	0.0506	0.1778	0.0592	0.2896	0.0771	0.5115	0.1190
$\sigma_M^2=0.5$	0.1280	0.0585	0.1795	0.0659	0.2344	0.0725	0.3463	0.0916	0.5647	0.1333
$\sigma_M^2=1.0$	0.2386	0.0886	0.2945	0.0962	0.3488	0.1048	0.4606	0.1242	0.6700	0.1618
$\sigma_M^2=2.0$	0.4685	0.1550	0.5210	0.1614	0.5723	0.1698	0.6752	0.1861	0.8781	0.2246

Table 3. ITAE in case of J_{TL} = 1 Nm

	$\sigma_P^2=0$, NF	$\sigma_P^2=0$, KF	$\sigma_P^2=0.25$, NF	$\sigma_P^2=0.25$, KF	$\sigma_P^2=0.5$, NF	$\sigma_P^2=0.5$, KF	$\sigma_P^2=1.0$, NF	$\sigma_P^2=1.0$, KF	$\sigma_P^2=2.0$, NF	$\sigma_P^2=2.0$, KF
$\sigma_M^2=0$	0.0475	0.0474	0.0863	0.0513	0.1383	0.0588	0.2501	0.0770	0.4737	0.1201
$\sigma_M^2=0.25$	0.0879	0.0568	0.1396	0.0639	0.1946	0.0726	0.3069	0.0902	0.5260	0.1323
$\sigma_M^2=0.5$	0.1423	0.0716	0.1966	0.0793	0.2524	0.0863	0.3644	0.1052	0.5823	0.1472
$\sigma_M^2=1.0$	0.2568	0.1022	0.3121	0.1099	0.3675	0.1187	0.4781	0.1384	0.6945	0.1761
$\sigma_M^2=2.0$	0.4863	0.1695	0.5366	0.1756	0.5900	0.1846	0.6984	0.2011	0.9088	0.2389

Table 4. ITAE in case of J_{TL} = 3 Nm

	$\sigma_P^2=0$, NF	$\sigma_P^2=0$, KF	$\sigma_P^2=0.25$, NF	$\sigma_P^2=0.25$, KF	$\sigma_P^2=0.5$, NF	$\sigma_P^2=0.5$, KF	$\sigma_P^2=1.0$, NF	$\sigma_P^2=1.0$, KF	$\sigma_P^2=2.0$, NF	$\sigma_P^2=2.0$, KF
$\sigma_M^2=0$	0.0762	0.0762	0.1127	0.0786	0.1635	0.0860	0.2698	0.1035	0.4881	0.1455
$\sigma_M^2=0.25$	0.1151	0.0848	0.1654	0.0918	0.2163	0.1002	0.3260	0.1168	0.5437	0.1566
$\sigma_M^2=0.5$	0.1688	0.1006	0.2187	0.1080	0.2728	0.1139	0.3820	0.1314	0.5980	0.1706
$\sigma_M^2=1.0$	0.2780	0.1322	0.3324	0.1391	0.3861	0.1465	0.4934	0.1641	0.7090	0.1989
$\sigma_M^2=2.0$	0.5042	0.1997	0.5571	0.2051	0.6089	0.2127	0.7166	0.2273	0.9465	0.2623

Table 5. ITAE in case of J_{TL} = 5 Nm

	$\sigma_P^2=0$, NF	$\sigma_P^2=0$, KF	$\sigma_P^2=0.25$, NF	$\sigma_P^2=0.25$, KF	$\sigma_P^2=0.5$, NF	$\sigma_P^2=0.5$, KF	$\sigma_P^2=1.0$, NF	$\sigma_P^2=1.0$, KF	$\sigma_P^2=2.0$, NF	$\sigma_P^2=2.0$, KF
$\sigma_M^2=0$	0.1014	0.1013	0.1410	0.1051	0.1959	0.1130	0.3077	0.1321	0.5333	0.1787
$\sigma_M^2=0.25$	0.1431	0.1122	0.1978	0.1192	0.2528	0.1278	0.3656	0.1474	0.5905	0.1922
$\sigma_M^2=0.5$	0.2010	0.1284	0.2551	0.1360	0.3108	0.1434	0.4223	0.1641	0.6494	0.2087
$\sigma_M^2=1.0$	0.3163	0.1624	0.3719	0.1712	0.4261	0.1803	0.5388	0.2001	0.7670	0.2420
$\sigma_M^2=2.0$	0.5496	0.2370	0.6058	0.2434	0.6631	0.2526	0.7749	0.2711	0.9962	0.3139

Table 6. ITAE in case of J_{TL} = 7 Nm

	$\sigma_P^2=0$, NF	$\sigma_P^2=0$, KF	$\sigma_P^2=0.25$, NF	$\sigma_P^2=0.25$, KF	$\sigma_P^2=0.5$, NF	$\sigma_P^2=0.5$, KF	$\sigma_P^2=1.0$, NF	$\sigma_P^2=1.0$, KF	$\sigma_P^2=2.0$, NF	$\sigma_P^2=2.0$, KF
$\sigma_M^2=0$	0.1280	0.1279	0.1664	0.1327	0.2179	0.1405	0.3282	0.1601	0.5635	0.2063
$\sigma_M^2=0.25$	0.1688	0.1398	0.2196	0.1465	0.2719	0.1550	0.3886	0.1740	0.6170	0.2187
$\sigma_M^2=0.5$	0.2228	0.1567	0.2742	0.1638	0.3308	0.1708	0.4489	0.1898	0.6725	0.2336
$\sigma_M^2=1.0$	0.3365	0.1914	0.3944	0.1987	0.4520	0.2066	0.5671	0.2249	0.7812	0.2633
$\sigma_M^2=2.0$	0.5771	0.2646	0.6283	0.2706	0.6824	0.2781	0.7889	0.2928	1.0198	0.3313

Table 7. ITAE in case of J_{TL} = 8 Nm

	$\sigma_P^2=0$, NF	$\sigma_P^2=0$, KF	$\sigma_P^2=0.25$, NF	$\sigma_P^2=0.25$, KF	$\sigma_P^2=0.5$, NF	$\sigma_P^2=0.5$, KF	$\sigma_P^2=1.0$, NF	$\sigma_P^2=1.0$, KF	$\sigma_P^2=2.0$, NF	$\sigma_P^2=2.0$, KF
$\sigma_M^2=0$	0.1413	0.1414	0.1801	0.1464	0.2311	0.1537	0.3424	0.1729	0.5704	0.2207
$\sigma_M^2=0.25$	0.1822	0.1543	0.2324	0.1607	0.2862	0.1688	0.4016	0.1879	0.6260	0.2344
$\sigma_M^2=0.5$	0.2360	0.1717	0.2885	0.1788	0.3454	0.1858	0.4604	0.2048	0.6905	0.2511
$\sigma_M^2=1.0$	0.3516	0.2085	0.4088	0.2161	0.4649	0.2241	0.5772	0.2437	0.8404	0.2845
$\sigma_M^2=2.0$	0.5926	0.2876	0.6521	0.2942	0.7154	0.3028	0.8690	0.3194	1.3613	0.3598

Table 8. ITAE in case of J_{TL} = 9 Nm

	$\sigma_P^2 = 0$, NF	$\sigma_P^2 = 0$, KF	$\sigma_P^2 = 0.25$, NF	$\sigma_P^2 = 0.25$, KF	$\sigma_P^2 = 0.5$, NF	$\sigma_P^2 = 0.5$, KF	$\sigma_P^2 = 1.0$, NF	$\sigma_P^2 = 1.0$, KF	$\sigma_P^2 = 2.0$, NF	$\sigma_P^2 = 2.0$, KF
$\sigma_M^2 = 0$	0.1554	0.1557	0.1944	0.1614	0.2504	0.1692	0.3884	0.1899	0.9126	0.2430
$\sigma_M^2 = 0.25$	0.1983	0.1712	0.2533	0.1783	0.3166	0.1871	0.4811	0.2081	1.3394	0.2600
$\sigma_M^2 = 0.5$	0.2588	0.1918	0.3228	0.1995	0.4024	0.2072	0.5922	0.2296	1.9711	0.2807
$\sigma_M^2 = 1.0$	0.4231	0.2365	0.5152	0.2458	0.6301	0.2558	1.0771	0.2778	3.6842	0.3267
$\sigma_M^2 = 2.0$	1.4037	0.3420	1.9313	0.3513	2.5949	0.3629	4.2353	0.3873	8.4152	0.4448

In order to evaluate the performance of simulated IM drive structures, the ITAE criterion is utilized. The ITAE index has the advantages of producing smaller overshoots and oscillations than the integral of the absolute error (IAE) or the integral square error (ISE) indices [34]. In this situation, it is modified according to (14):

$$ITAE = \int_0^2 t|e_\omega(t)|dt \quad (14)$$

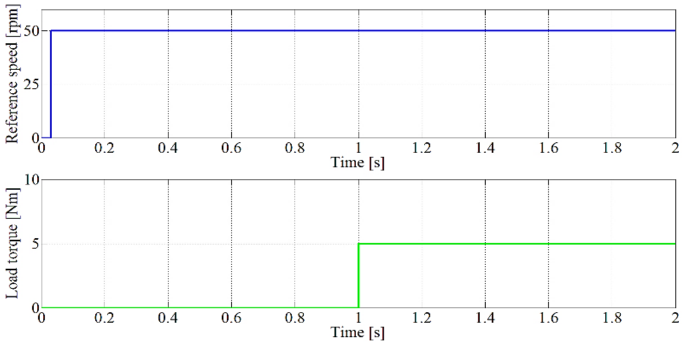

Figure 2. Reference speed (upper), and load torque with J_{TL} = 5 Nm

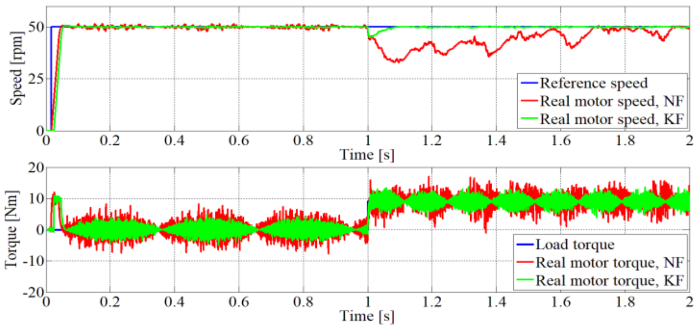

Figure 3. Speeds (upper), and torques with J_{TL} = 9 Nm, $\sigma_P^2 = 2$, $\sigma_M^2 = 2$

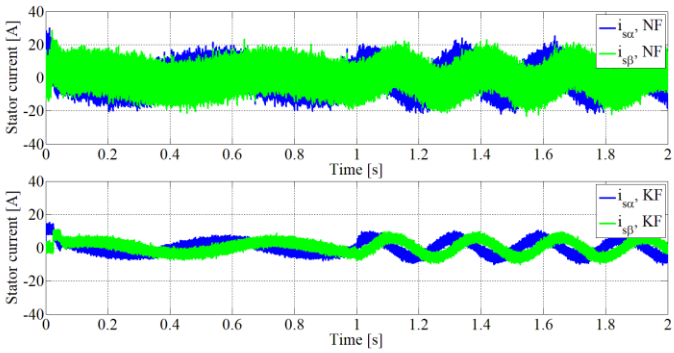

Figure 4. Stator currents with NF (upper) and KF with J_{TL} = 9 Nm, $\sigma_P^2 = 2$, $\sigma_M^2 = 2$

It is easy to see that starting duration for NF is shorter than that for KF (see Figure 3). The reason for this problem is Kalman filter reduces ripple of stator current (see Figure 4) and even ripple of stator flux (see Figure 5), and therefore, it lengthens process of reaching rated value of stator flux and limit of stator current. In Figure 2, at time of load activation, large negative instantaneous deviation of motor torque and load torque makes motor speed decrease quickly for both NF and KF. After this time, for NF, unfiltered stator currents continue to give high ripple of motor torque which indirectly lengthens this decrement (see Figure 3). Undershoot after load activation of speed responses for NF and KF is 17.2 rpm and 5.1 rpm respectively. Ripples of stator flux magnitude in the first and second half of the course (FSHC) for KF are 6.0% and 8.8% smaller respectively than those for NF. Motor torque ripple in the FSHC for KF are reduced by 39.9% and 25.7% compared to those for NF. Especially, ripple of stator current magnitude in the FSHC for KF is 3.3 times and 2.6 times lower respectively than those for NF.

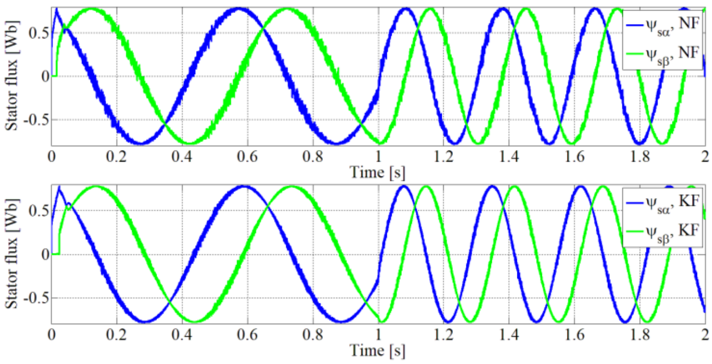

Figure 5. Stator fluxes with NF (upper) and KF with J_{TL} = 9 Nm, $\sigma_P^2 = 2$, $\sigma_M^2 = 2$

4. CONCLUSIONS

The PWM-DTC IM drive structure using simplified Kalman filter for stator current filtration in case of unknown IM model was presented in the paper. Simulations were carried out with different values of load torque jump, noise covariances. The proposed drive structure gave significantly smaller ITAE performance index than the conventional drive structure, especially at high levels of noise covariances. The EKF or UKF with knowledge of IM mathematical model can be utilized to obtain higher filtration efficiency. Robust control, intelligent control or sensorless control techniques can be applied for IM drive with filtered stator current components.

REFERENCES

[1] P. Vas, “Sensorless Vector and Direct Torque Control,” *Oxford: Oxford University Press*, 1998.
[2] P. Brandstetter, *et al.*, “Induction motor drive with PWM direct torque control,” *2017 18th International Scientific Conference on Electric Power Engineering (EPE)*, pp. 1-5, May 2017.
[3] S. S. Hakami, I. M. Alsofyani and K. Lee, “Torque ripple reduction and flux-droop minimization of DTC with improved interleaving CSFTC of IM Fed by three-level NPC inverter,” *IEEE Access*, vol. 7, pp. 184266-184275, December 2019.
[4] M. Depenbrock, “US4678248 direct self-control of the flux and rotary moment of a rotary-field machine,” *United States Patent*, October 1984.
[5] M. Depenbrock, “DE3438504 (A1) - Method and Device for Controlling of a Rotating Field Machine,” *European Patent Office*, October 1984.
[6] I. Takahashi, T. Noguchi, "A new quick-response and high-efficiency control strategy of an induction motor,” *IEEE Transactions on Industry Applications*, vol. IA-22, no. 5, pp. 820-827, September 1986.
[7] B. S. Kumar, R. A. Gupta, R. Kumar, “12-sector methodology of torque ripple reduction in a direct torque controlled induction motor drive,” *2006 SICE-ICASE International Joint Conference*, pp. 3587-3592, October 2006.
[8] P. Brandstetter, P. Chlebis and P. Palacky, “Direct torque control of induction motor with direct calculation of voltage vector,” *Advances in Electrical and Computer Engineering*, vol. 10, no. 4, pp.17-22, November 2010.
[9] S. A. Vaezi, H. Iman-Eini and R. Razi, “A new space vector modulation technique for reducing switching losses in induction motor DTC-SVM scheme,” *2019 10th International Power Electronics, Drive Systems and Technologies Conference (PEDSTC)*, pp. 184-188, February 2019.
[10] R. E. Kalman, “A new approach to linear filtering and prediction problems,” *Transactions of the ASME*, *Journal of Basic Engineering*, vol. 82, no. 1, pp. 35-45, 1960.

[11] R. E. Kalman and R. S. Bucy, "New results in linear filtering and prediction theory," *Transactions of the ASME, Journal of Basic Engineering*, vol. 83, no. 1, pp. 95-108, March 1961.
[12] F. Auger*, et al.*, "Industrial applications of the Kalman filter: A review," *IEEE Transactions on Industrial Electronics*, vol. 60, no. 12, pp. 5458-5471, December 2013.
[13] S. Peng*, et al.*, "State of charge estimation of battery energy storage systems based on adaptive unscented Kalman filter with a noise statistics estimator," *IEEE Access*, vol. 5, pp. 13202-13212, July 2017.
[14] H. Ahmad, N. A. Othman and M. S. Ramli, "A solution to partial observability in extended kalman filter mobile robot navigation," *TELKOMNIKA Telecommunication Computing Electronics and Control*, vol. 16, no. 1, pp. 134-141, February 2018.
[15] S. N. A. M. Amin*, et al.*, "Kalman filter estimation of impedance parameters for medium transmission line," *TELKOMNIKA Telecommunication Computing Electronics and Control*, vol. 16, no. 2, pp. 900-908, April 2018.
[16] P. B. Solanki, M. Al-Rubaiai and X. Tan, "Extended Kalman filter-based active alignment control for LED optical communication," *IEEE/ASME Transactions on Mechatronics*, vol. 23, no. 4, pp. 1501-1511, August 2018.
[17] Z. Lin, H. H. T. Liu and M. Wotton, "Kalman filter-based large-scale wildfire monitoring with a system of UAVs," *IEEE Transactions on Industrial Electronics*, vol. 66, no. 1, pp. 606-615, January 2019.
[18] J. Hakkarainen*, et al.*, "Undersampled dynamic X-Ray tomography with dimension reduction Kalman filter," *IEEE Transactions on Computational Imaging*, vol. 5, no. 3, pp. 492-501, September 2019.
[19] B. A. McElhoe, "An assessment of the navigation and course corrections for a manned flyby of mars or venus," *IEEE Transactions on Aerospace and Electronic Systems*, vol. AES-2, no. 4, pp. 613-623, July 1966.
[20] S. J. Julier and J. K. Uhlmann, "New extension of the Kalman filter to nonlinear systems," *Proc. SPIE 3068, Signal Processing, Sensor Fusion, and Target Recognition VI*, pp. 182-193, July 1997.
[21] P. K. Kitanidis, "Unbiased minimum-variance linear state estimation," *Automatica*, vol. 23, no. 6, pp. 775-778, November 1987.
[22] D. Varshney, M. Bhushan and S. C. Patwardhan, "State and parameter estimation using extended kitanidis Kalman filter," *Journal of Process Control*, vol. 76, pp. 98-111, April 2019.
[23] E. Zerdali and M. Barut, "The comparisons of optimized extended Kalman filters for speed-sensorless control of induction motors," *IEEE Transactions on Industrial Electronics*, vol. 64, no. 6, pp. 4340-4351, June 2017.
[24] K. S. Xiahou, X. Lin and Q. H. Wu, "Current sensor fault-tolerant control of DFIGs using stator current regulators and Kalman filter," *2017 IEEE Power & Energy Society General Meeting*, pp. 1-5, July 2017.
[25] A. A. Tanvir and A. Merabet, "Artificial neural network and Kalman filter for estimation and control in standalone induction generator wind energy DC microgrid," *Energies*, vol. 13, no. 7, April 2020.
[26] U. Syamkumar and B. Jayanand, "A reduced order smoothing filter for speed estimation of three phase induction motor," *TENCON 2017 - 2017 IEEE Region 10 Conference*, pp. 1749-1754, November 2017.
[27] A. Chahmi and A. Djoudi, "Diagnosis of the induction machine by the Kalman filter," *2017 5th International Conference on Electrical Engineering - Boumerdes (ICEE-B)*, pp. 1-7, October 2017.
[28] J. Mohana Lakshmi and H. N. Suresh, "Accuracy improvement of induction motor speed estimation using improvised tuning of extended Kalman filter technique," *2018 IEEE 13th International Conference on Industrial and Information Systems (ICIIS)*, pp. 395-400, 2018.
[29] K. Horváth, "Cubature Kalman filter-based speed sensorless control of induction machines," *2018 20th International Symposium on Electrical Apparatus and Technologies (SIELA)*, pp. 1-4, June 2018.
[30] E. Zerdali, "Adaptive extended kalman filter for speed-sensorless control of induction motors," *IEEE Transactions on Energy Conversion*, vol. 34, no. 2, pp. 789-800, June 2019.
[31] A. Taheri, H. Ren and M. H. Holakooie, "Sensorless loss model control of the six-phase induction motor in all speed range by extended Kalman filter," *IEEE Access*, vol. 8, pp. 118741-118750, January 2020.
[32] R. Yildiz, M. Barut and E. Zerdali, "A comprehensive comparison of extended and unscented Kalman filters for speed-sensorless control applications of induction motors," *IEEE Transactions on Industrial Informatics*, vol. 16, no. 10, pp. 6423-6432, October 2020.
[33] A. O'Dwyer, "Handbook of PI and PID controller tunning rules," *London: Imperial College Press*, 2009.
[34] D. Maiti*, et al.*, "Tuning PID and PI/λDδ controllers using the integral time absolute error criterion," *2008 4th International Conference on Information and Automation for Sustainability*, pp. 457-462, 2008.

BIOGRAPHIES OF AUTHORS

Hau Huu Vo hold a PhD degree from Technical University of Ostrava (VSB-TUO), Czech Republic in 2017. He has been working as a Lecturer at Faculty of Electrical and Electronics Engineering (FEEE), Ton Duc Thang University (TDTU), Vietnam. He has published 10 conference papers and 5 journal papers. His current research interests are intelligent electrical drives, control theory and robotics.

Dung Quang Nguyen received his MSc degree from Tomsk Polytechnic University, Tomsk City, Russia in 2012. He is now a PhD Student at FEEE, TDTU, Vietnam. His research interests include applications of Kalman filter in control systems; identification and synthesis in fractional, distributed parameter systems; non-linear system; PLC and SCADA system, industrial communication networks, image processing.

Quang Thanh Nguyen hold his MSc degree from TDTU, Vietnam in 2019. He is preparing to become a PhD Student at FEEE, TDTU, Vietnam. His research interests include applications of intelligent control in electrical drives, microcontroller, robotics, SCADA.

Chau Si Thien Dong obtained her PhD degree from VSB-TUO, Czech Republic in 2017. She is now dean of FEEE, TDTU, Vietnam. She has published 15 conference papers and 5 journal papers. Her research interests focus on modern control and drives.

Thinh Cong Tran completed his PhD degree at VSB-TUO, Czech Republic in 2018. He serves as a Lecturer at FEEE, TDTU, Vietnam. He has published 8 conference papers and 4 journal papers. His research interests are microcontroller systems and intelligent electrical drives.

Pavel Brandstetter has completed his PhD degree at Brno University in 1987. He is now full professor and dean of Faculty of Electrical Engineering and Computer Science at VSB-TUO, Czech Republic. He has published more than 50 conference papers and 25 journal papers. His research interests are intelligent methods in power electronics and electrical drives.